Research Paper

Sulfate assimilation regulates hydrogen sulfide production independent of lifespan and reactive oxygen species under methionine restriction condition in yeast

Kyung-Mi Choi[1,*], Sorah Kim[1,*], Seahyun Kim[1], Hae Min Lee[1], Alaattin Kaya[2], Bok-Hwan Chun[1], Yong Kwon Lee[3], Tae-Sik Park[4], Cheol-Koo Lee[1], Seong-il Eyun[5], Byung Cheon Lee[1]

[1]College of Life Sciences and Biotechnology, Korea University, Seoul 02841, Republic of Korea
[2]Division of Genetics, Department of Medicine, Brigham & Women's Hospital and Harvard Medical School, Boston, MA 02115, USA
[3]Department of Culinary Art and Food Service Management, Yuhan University, Bucheon 422-749, Republic of Korea
[4]Department of Life Science, Gachon University, Sungnam, Republic of Korea
[5]Department of Life Science, Chung-Ang University, Seoul, Republic of Korea
[*]Equal contribution

Correspondence to: Byung Cheon Lee; **email:** cheonii@korea.ac.kr
Keywords: high-throughput genetic screening, methionine restriction, hydrogen sulfide, sulfate assimilation, reactive oxygen species
Received: January24, 2019 **Accepted:** June 18, 2019 **Published:** June 29, 2019

Copyright: Choi et al. This is an open-access article distributed under the terms of the Creative Commons Attribution License (CC BY 3.0), which permits unrestricted use, distribution, and reproduction in any medium, provided the original author and source are credited.

ABSTRACT

Endogenously produced hydrogen sulfide was proposed to be an underlying mechanism of lifespan extension via methionine restriction. However, hydrogen sulfide regulation and its beneficial effects via methionine restriction remain elusive. Here, we identified the genes required to increase hydrogen sulfide production under methionine restriction condition using genome-wide high-throughput screening in yeast strains with single-gene deletions. Sulfate assimilation-related genes, such as *MET1*, *MET3*, *MET5*, and *MET10*, were found to be particularly crucial for hydrogen sulfide production. Interestingly, methionine restriction failed to increase hydrogen sulfide production in mutant strains; however, it successfully extended chronological lifespan and reduced reactive oxygen species levels. Altogether, our observations suggested that increased hydrogen sulfide production via methionine restriction is not the mechanism underlying extended yeast lifespan, even though increased hydrogen sulfide production occurred simultaneously with yeast lifespan extension under methionine restriction condition.

INTRODUCTION

Caloric restriction (CR) has been successfully shown to extend lifespans in various laboratory models [1]. The latest collaborative study between the National Institute on Aging and University of Wisconsin Madison involving rhesus monkeys reported an improvement in survival via CR [2]. Moreover, recent clinical trial in humans examined the effect of CR with respect to two well-known aging theories (rate of living and oxidative damage), which showed promising results in promoting human health by 2-year-CR [3]. However, despite sufficient evidence demonstrating CR-mediated longevity, it is difficult to maintain reduced caloric intake during an entire human lifetime. Thus, alternative strategies that mimic the CR effect without reducing

total energy intake have been investigated. One of these strategies is methionine restriction (MR), a regimen that only limits nutritional access to methionine.

MR-mediated lifespan extension has been reported in short-lived organisms, including *Saccharomyces cerevisiae* (budding yeast) [4-7]. Two types of aging models exist in budding yeast: the replicative lifespan model measures the number of daughter cells produced by mother cells; and the chronological lifespan (CLS) model measures the survival time of populations during the stationary phase and is widely accepted as a model for postmitotic cell aging in higher organisms [8]. A recent study [9] showed that methionine-auxotroph yeasts (exhibiting defective *de novo* methionine biosynthesis) have longer CLS than prototroph strains capable of synthesizing methionine. In the same study, higher level of external methionine was observed to decrease CLS, whereas MR was shown to increase it.

Although the lifespan-extending effect of MR is well established across different species, not much is known about the mechanism of action by which MR elicits longevity. Recently Hine and coworkers [10] suggested CR-induced increased hydrogen sulfide production as a molecular mediator for CR-mediated lifespan extension. Hydrogen sulfide is produced via the transsulfuration pathway (TSP) enzymes, cystathionine β-synthase (CBS) and cystathionine γ-lyase (CGL). These enzymes are evolutionarily conserved across eukaryotes including yeast i.e., *CYS3* and *CYS4* encode *CGL* and *CBS*, respectively [11, 12]. In addition to the TSP, a yeast-specific sulfate assimilation pathway also catalyzes extracellular sulfates into intracellular

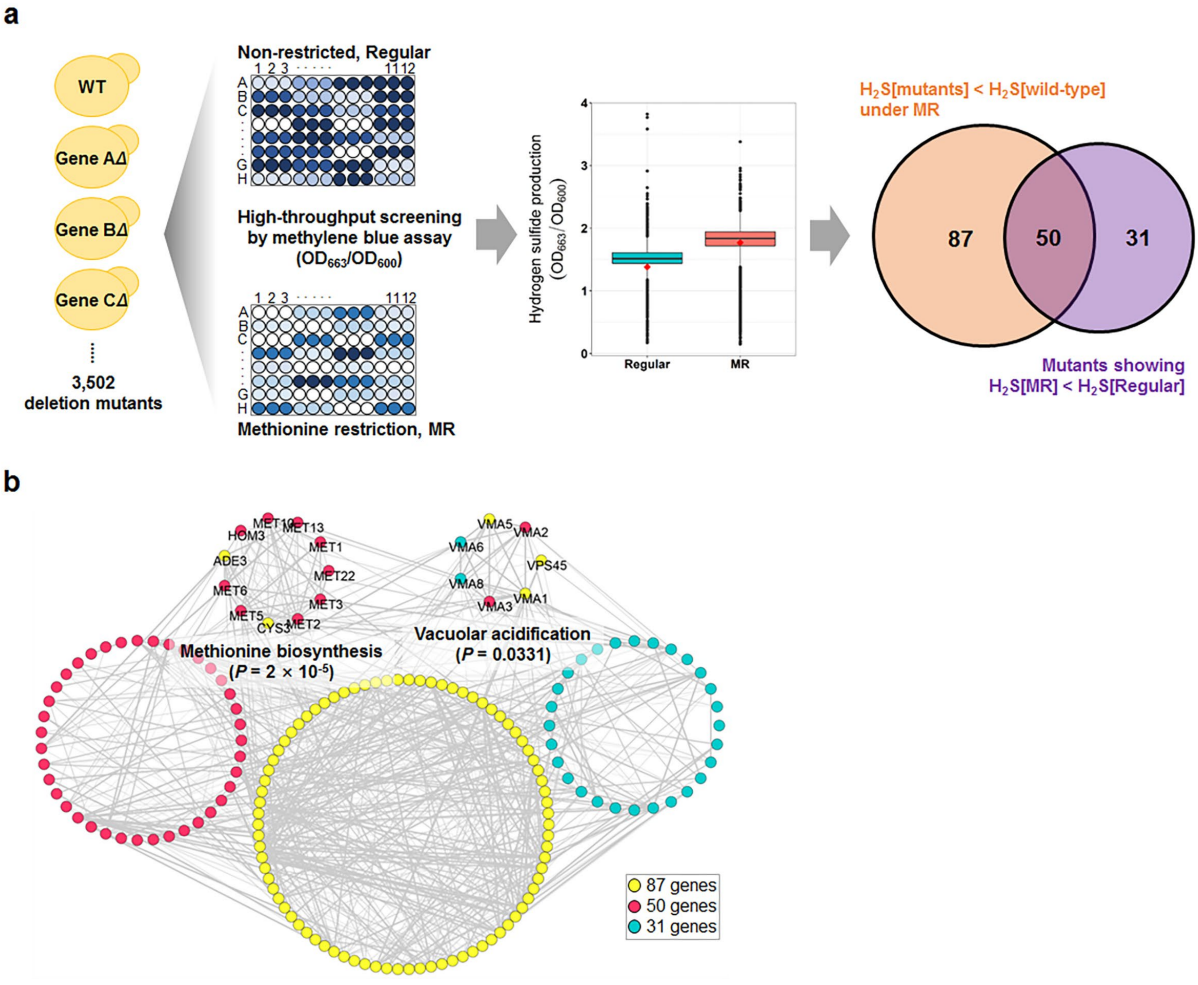

Figure 1. Genome-wide screening for genes involved in hydrogen sulfide production under MR condition. (**a**) Schematic screening strategy and hydrogen sulfide levels of total screening genes under regular and MR condition at 15 h after inoculation. The red diamond in the box plot indicates the value of the wild-type strain. The Venn diagram shows the number of mutants selected by 2 different statistical strategies. (**b**) Genetic network of the 168 selected genes from 2 analyses. The significantly enriched biological processes and involved genes are indicated.

hydrogen sulfide. Once CR is induced in yeast (achieved by reducing glucose level from 2% to 0.5% in culture media), endogenous hydrogen sulfide production is observed to increase [10]. Interestingly, yeast strains lacking the assimilation pathway genes (*met5Δ*, *met14Δ*, and *met16Δ*) in 2% glucose media demonstrate decreased hydrogen sulfide levels. However, increased hydrogen sulfide via CR is still maintained in these mutants, thus implying the minimal involvement of the sulfur assimilation pathway in inducing hydrogen sulfide under CR conditions [10]. Given that MR and CR enhance longevity via nutrient restriction, we wondered whether MR possibly employed hydrogen sulfide to extend lifespan.

The goal of this study was to identify the genes or pathways that control hydrogen sulfide production under MR condition and to determine the role of hydrogen sulfide in lifespan extension. We investigated hydrogen sulfide production in nearly 3,500 knockout strains under regular or MR conditions using unbiased genome-wide high-throughput genetic screening. In contrast to that in CR conditions, we determined sulfate assimilation genes to be critical in increasing hydrogen sulfide production under MR condition. Furthermore, hydrogen sulfide induction was not associated with lifespan extension and decreased reactive oxygen species (ROS) under the MR condition. Altogether, this study suggests that the cellular function of hydrogen sulfide varies based on nutritional status, which may point out the difference between MR and CR while determining mechanisms for longevity.

RESULTS

High-throughput genetic screening-based identification of genes required for hydrogen sulfide production under MR condition

MR induces lifespan extension and triggers an increase in endogenous hydrogen sulfide levels [13]. Hydrogen sulfide is particularly considered to be an essential mediator of MR benefits; however, its role in MR still remains unclear. To address this, we exploited an MR media that was previously shown to extend the lifespan of yeast [6]. This MR media was first used to examine the change in hydrogen sulfide production in the presence of different methionine concentrations using a lead acetate paper assay. As expected, hydrogen sulfide production was observed to be consistently higher in yeast cells grown using MR media when compared to those grown using regular media (Fig. S1).

Next, we conducted high-throughput hydrogen sulfide screening for the MR media with the yeast knockout collection (Fig. 1a). For this screening process, we used the methylene blue assay, in which the blue color changes to colorless upon hydrogen sulfide production. During this screening, two optical densities were measured simultaneously; one at OD_{663} to determine hydrogen sulfide production and another at OD_{600} to determine cell mass. These measurements were then used to calculate hydrogen sulfide production per cell. Compared to that in regular media, most of the tested strains, including wild-type, consistently showed low cell mass during the stationary phase (Fig. S2) and increased hydrogen sulfide production (Fig. 1a) in the MR media. Consequently, average hydrogen sulfide production per cell dramatically increased in the MR media. To identify the genes that regulated the increase in hydrogen sulfide production under the MR condition, two analytical strategies were applied to the screening data (Fig. 1a): 137 deletion mutant strains were selected to produce lesser hydrogen sulfide than the wild-type in MR media (Table S2; fold-change < -1.5; FDR-adjusted p-value < 0.05) and 81 deletion mutant stains were selected to exhibit no increase in hydrogen sulfide production under MR condition (Table S3; hydrogen sulfide production ratio between MR and regular media < 1; FDR-adjusted p-value < 0.05). Interestingly, 50 genes resided in the intersection between two independently performed comparisons (Fig. 1a). Next, we carried out Gene Ontology analysis for a total of 168 genes obtained from both analyses and found that genes involved in methionine biosynthesis (11 genes; p-value = 0.0000) and vacuolar acidification (7 genes; p-value = 0.0331) were significantly enriched (Fig. 1b). Therefore, we surmised that these two pathways (methionine biosynthesis and vacuolar acidification) possibly played a role in regulating hydrogen sulfide production under MR condition.

Deletion of *MET1*, *MET3*, *MET5* or *MET10* reduces hydrogen sulfide production under MR condition

Based on the high-throughput methylene blue assay, methionine biosynthesis and vacuolar acidification were predicted to be involved in the regulation of hydrogen sulfide production under MR condition. Next, an alternative hydrogen sulfide detection assay was further performed to confirm these results owing to the pH dependency of methylene blue color change. Thus, we measured hydrogen sulfide production in deletion mutant strains associated with methionine metabolism (Fig. 2a) and vacuolar acidification under various methionine concentrations (50, 25, 12.5, and 5 mg/L) using lead acetate assay (Fig. 2b, S3, and S4). Methionine concentration showed a strong negative correlation with hydrogen sulfide production in wild-type yeast cells (Fig. 2b), which indicated reduced methionine uptake to be very effective in increasing hydrogen sulfide production. This phenomenon was

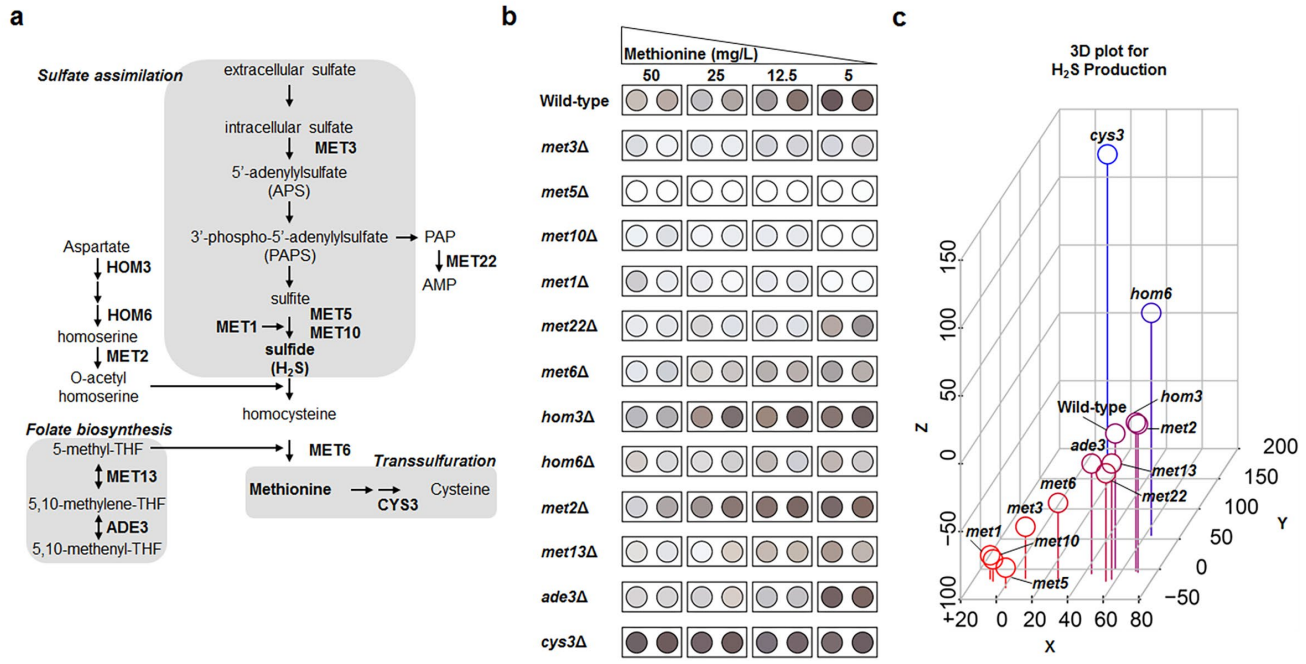

Figure 2. Genes involved in sulfate assimilation are crucial for MR-mediated H_2S production. (**a**) Methionine metabolic pathway. A gene name is shown in the corresponding step. (**b**) Lead acetate assay to determine methionine metabolism-related genes under diverse methionine restricted conditions. (**c**) Three-dimensional plot demonstrating the effect of gene deletion on hydrogen sulfide production. Hydrogen sulfide levels under 50 mg/L (regular condition) and 5 mg/L (MR condition) of methionine were digitized based on spot darkness. For wild-type and deletion mutants, the x-axis indicates the difference between MR-condition and regular-condition hydrogen sulfide levels and the y- and z-axes indicate the difference between the deletion mutant and wild-type hydrogen sulfide levels under regular and MR conditions, respectively. Spot color shows low (red) to high (blue) z-axis values.

also observed in most deletion mutant strains whose vacuolar acidification pathway genes were knocked out (Fig. S4). In contrast, all deletion mutant strains associated with sulfate assimilation, including *met1Δ*, *met3Δ*, *met5Δ*, and *met10Δ*, failed to increase hydrogen sulfide production to wild-type levels under MR conditions (Fig. 2b). These differences in hydrogen sulfide production were analyzed in following 3 ways and are shown in the 3D plot (Fig. 2c). For each strain, we subtracted the hydrogen sulfide amounts under regular condition from those under MR condition ($[H_2S]_{MR} - [H_2S]_{Reg}$; x-axis). For regular condition, we subtracted the wild-type hydrogen sulfide amount from each deletion mutant hydrogen sulfide amount ($[H_2S]_{mutant\ in\ regular} - [H_2S]_{WT\ in\ regular}$; y-axis). The values for z-axis ($[H_2S]_{mutant\ in\ MR} - [H_2S]_{WT\ in\ MR}$) were calculated in the same way as those for the y-axis, except that they were obtained under MR condition. Interestingly, the four deletion mutant strains exhibiting defective sulfate assimilation were observed in the bottom left corner of the 3D plot, thus showing greatly reduced hydrogen sulfide production when compared to the wild-type under MR condition. Consequently, it also meant that the sulfate assimilation pathway was crucial for increasing hydrogen sulfide production under MR condition. Therefore, we surmised that the sulfate assimilation pathway may possibly have a regulatory role in upregulating hydrogen sulfide production when methionine uptake is reduced.

Increased hydrogen sulfide production is not directly associated with lifespan extension of yeast under the MR condition

MR mimics many aspects of CR-mediated benefits, including lifespan extension and increased hydrogen sulfide production [10, 13]. Increased hydrogen sulfide levels are particularly considered to be a mediator of lifespan extension under CR condition. In this regard, we assessed the effect of increased hydrogen sulfide production on lifespan under MR condition. Previously, DeLuna and his colleagues identified yeast aging genes from the stationary phase survival data of yeast single gene knockout mutants using an automated chronological lifespan assay [14]. Upon correlating our hydrogen sulfide production data against this genome-wide chronological lifespan data, no significant correlation between hydrogen sulfide production and lifespan was observed in the deletion mutant strains (correlation value was -0.009 and -0.151 under regular

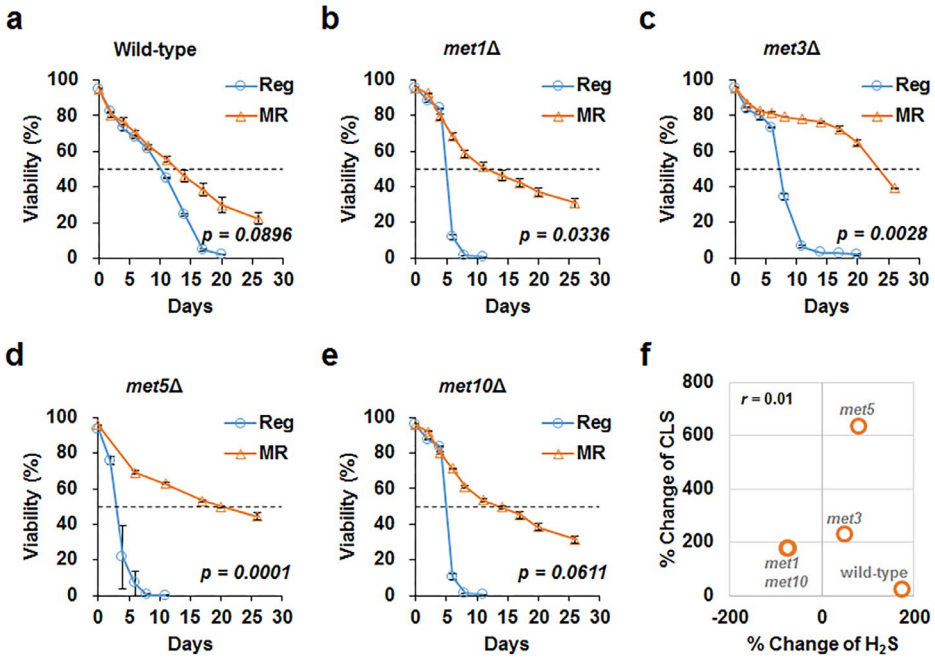

Figure 3. MR successfully increases CLS despite defective sulfur assimilation. CLS measured under regular (blue line) and MR (orange line) conditions in wild-type (**a**), *met1Δ* (**b**), *met3Δ* (**c**), *met5Δ* (**d**), and *met10Δ* (**e**) strains. The horizontal dotted line represents 50% viability. The graph indicates mean ± SEM. Statistical p-values between median CLS in regular and MR condition were calculated using two-tailed Student's *t*-test. (**f**) For each strain, we plotted the change in hydrogen sulfide levels (x-axis) and change in CLS (y-axis) under MR conditions against regular condition. The Pearson's correlation coefficient (r) was observed to be 0.01.

and MR conditions; Fig. S5). To demonstrate this experimentally, deletion mutants that exhibited defective sulfur assimilation and failed to increase hydrogen sulfide production in MR media were examined. Although these deletion mutants showed shorter lifespans than the wild-type in regular media, their lifespans were observed to extend at par with that of the wild-type under MR condition (Fig. 3 and Table. S3). As a result, MR-mediated lifespan extension was concluded to be maintained independent of hydrogen sulfide production in all tested deletion mutants (Fig. 3f).

To better understand the role of hydrogen sulfide in lifespan, we added a hydrogen sulfide donor, sodium hydrosulfide (NaHS), to wild-type cells grown in regular and MR media, i.e., the cells were treated thrice (6, 24, and 48 h after inoculation) with 5 μM NaHS. However, lifespan was not observed to extend by adding this small concentration of NaHS under both regular and MR conditions (Fig. S6). Next, we tested the effect of a much higher concentration of NaHS (50 μM) on wild-type, *met3Δ*, and *met5Δ* strains at the culture starting point (Fig. 4 and S7). Whereas NaHS markedly increased hydrogen sulfide production, lifespan remained unchanged after NaHS treatment in all tested strains under regular and MR conditions. Therefore, we concluded that increased extracellular hydrogen sulfide production was not directly related to lifespan extension under the MR condition.

Recent studies suggested that hydrogen sulfide protected cells from oxidative stress by reducing ROS or increasing antioxidant production [15]. Hence, we examined the relation between ROS and MR-mediated lifespan extension and hydrogen sulfide production. Under regular condition, deletion mutants produced about 2 to 6-fold higher ROS levels than the wild-type (Fig. 5). However, no noticeable difference in the ROS levels was observed between mutants and the wild-type upon methionine restriction (Fig. 5). Thus, all strains, including the wild-type and deletion mutants, showed decreased ROS levels via MR. Although this suggested a relation between MR-mediated decrease in ROS levels and lifespan extension under MR condition, it did not necessarily associate the process with changes in hydrogen sulfide production via MR.

DISCUSSION

In this study, we demonstrated that MR promotes hydrogen sulfide production similar to CR [10]. However, unlike CR, the induced hydrogen sulfide does

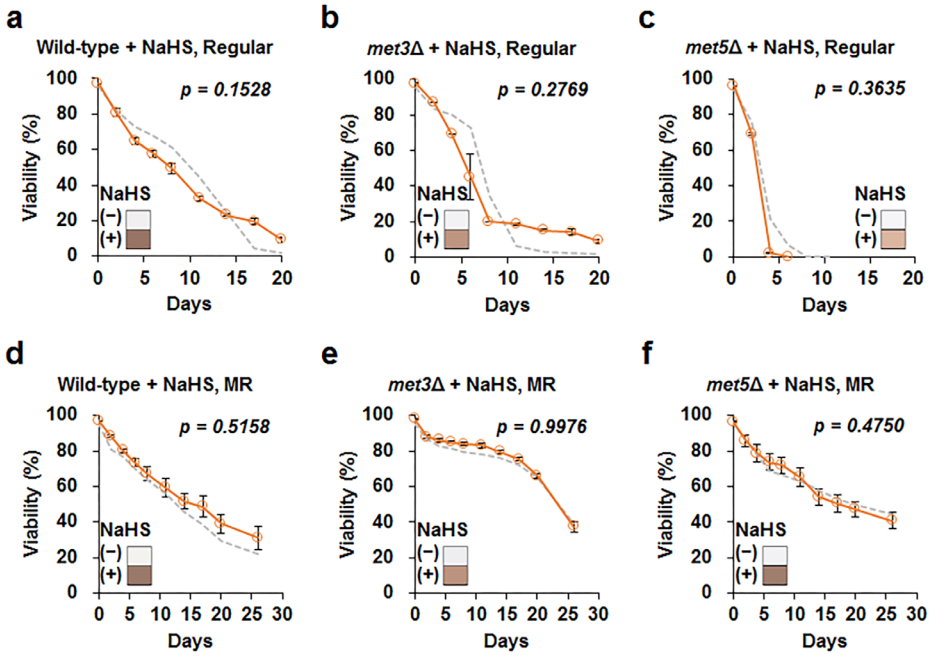

Figure 4. Increase in exogenous H_2S does not affect cellular lifespan. Lifespan after addition of 50 μM sodium hydrosulfide (NaHS) at culture starting points (orange line) in wild-type, *met3Δ*, and *met5Δ* strains under regular (**a** to **c**) and MR (**d** to **f**) conditions. The graph indicates mean ± SEM. The gray dotted line indicates CLS without NaHS for each strain shown in Fig. 3. Statistical p-value between median CLS before and after NaHS addition was calculated using two-tailed Student's *t*-test. The hydrogen sulfide levels measured using lead acetate paper is shown in the corner of the graph (original images are provided in Fig. S7).

not correlate with lifespan extension via MR, thus questioning the beneficial effects of MR on longevity via hydrogen sulfide production.

As a systematic approach to identifying genes involved in hydrogen sulfide production under MR condition, we screened nearly 3,500 knockouts in the BY4741 yeast genetic background. Both, a methylene blue assay for genetic screening (Fig. 1) and a sensitive lead-acetate assay (Fig. 2) allowed us to observe the positive role of the sulfate assimilation pathway in hydrogen sulfide production under MR condition. Sulfate assimilation-deficient strains showed a drastic reduction in hydrogen sulfide production when compared to the wild-type strain under both MR and regular conditions. However, the effect of deletion of the sulfate assimilation genes with respect to hydrogen sulfide production was much stronger under MR condition. Furthermore, a gradual increase in hydrogen sulfide levels along with an increase in the MR extent was abolished in deletion strains defective for sulfur assimilation (Fig. 2). Previously, *MET1* and *MET5* gene expression was reported to be induced upon methionine limitation [16]. Based on this report, we surmise that sulfur assimilation-related gene transcription may be induced and the pathway leading to *de novo* methionine biosynthesis may also be activated when methionine supplementation is reduced. This may be a cellular adaptation process to compensate for the low intracellular methionine levels. As a result, this may increase hydrogen sulfide levels, which is produced during the process of converting extracellular sulfate to homocysteine. In this context, cells lacking sulfate assimilation genes may fail to activate the sulfate assimilation pathway, thereby resulting in decreased hydrogen sulfide production under MR condition.

Although our initial screening data also showed the involvement of vacuolar acidification in regulating hydrogen sulfide production under MR condition (Fig. 1b), this process was not identified in the lead-acetate assay (Fig. S4), thus suggesting that pH variation caused by vacuolar acidification gene deletion may have influenced the methylene blue assay results. Intriguingly, a recent study suggested that autophagy-dependent vacuolar acidification was required for lifespan extension via MR [9]. Disruption of vacuolar acidification via *ATG5* deletion in the methionine-auxotrophic *met2Δ* strain (*met2Δatg5Δ*) abolished lifespan extension in the *met2Δ* strain when compared with that in the methionine-prototrophic MET^+ strain. Furthermore, overexpression of vacuole ATPases,

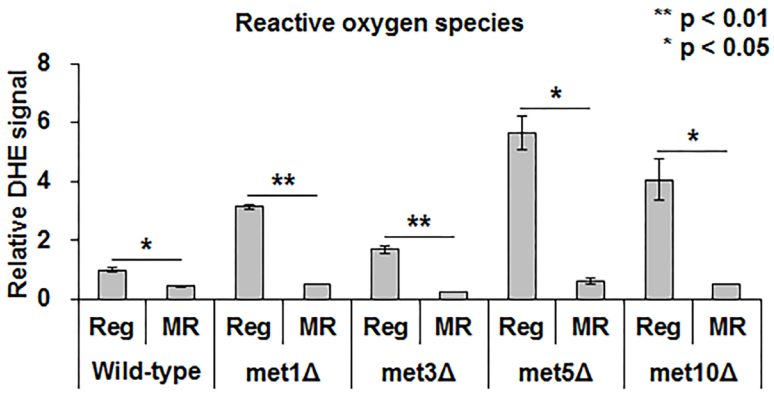

Figure 5. MR significantly reduces ROS regardless of methionine assimilation defectiveness. ROS levels in the wild-type strain under regular condition is considered as the standard. The relative level of the other strains is depicted. Experiments were run in triplicate. The bar graph indicates the mean ± SEM. The asterisks (*) indicate the p-value calculated using two-tailed Student's *t*-test between regular and MR conditions in the same strain.

including *VMA1* and *VPH2* (which leads to vacuole acidification), increased CLS in the MET^+ strain and did not extend the lifespan in *met2Δ*, thus suggesting the promotion of MR-mediated longevity via enhanced vacuolar acidity. However, no difference in hydrogen sulfide production under MR condition was observed between the wild-type and various deletion mutants devoid of vacuolar acidification (Fig. S4). Thus, our data again pointed out that MR likely extended yeast lifespan independent of hydrogen sulfide.

In animals, the breakdown of cysteine via *CBS* and *CSE* is crucial for hydrogen sulfide production; therefore, those two genes play a role in controlling endogenous hydrogen sulfide production. In yeast, *CYS3* and *CYS4* are orthologs of mammalian *CSE* and *CBS*, respectively. Interestingly, hydrogen sulfide production in *cys3Δ* (Fig. 2b) and *cys4Δ* was higher than that in the wild-type under both regular and MR condition [17]. Consequently, it suggests that the defective cysteine catabolism may be related to the upregulation of sulfate assimilation in order to compensate for hydrogen sulfide production. Importantly, sulfate assimilation via sulfite reductase is not conserved in animal, while cysteine catabolism via *CBS* and *CSE* acts as the main source of hydrogen sulfide [18]. Thus, we hypothesize that a different strategy might be adopted to regulate hydrogen sulfide production in yeast under MR condition and it might be the reason why increased hydrogen sulfide production by MR is not the mechanism underlying extended yeast lifespan.

Previously, hydrogen sulfide was suggested to alleviate oxidative stress levels by reducing ROS generation [19, 20]. However, our data (Fig. 5) showed that ROS generation under MR condition remained consistently low regardless of hydrogen sulfide levels, thereby supporting the idea that yeast, unlike mammals, utilize a different mechanism to regulate hydrogen sulfide production under MR condition. Consistently, lifespan extension also does not correlate with the regulation of hydrogen sulfide production under MR condition (Fig. 3 and 4). In conclusion, yeast uses a different strategy, such as sulfate assimilation, to increase its hydrogen sulfide production against methionine deficiency, which is independent of longevity and ROS generation. Future work involving an unbiased systematic approach in other species should be carried out to further clarify the origins of the beneficial effects of MR.

MATERIALS AND METHODS

Yeast strains and culture media

Saccharomyces cerevisiae BY4741 (MATa *his3Δ*1 *leu2Δ*0 *met15Δ*0 *ura3Δ*0) and deletion strain collections (BY4741 background) were used in this study (EUROSCARF, Germany). Unless otherwise noted, yeast cells were grown in synthetic medium (Table S4) containing 50 mg/L or 5 mg/L of methionine for regular and MR conditions, respectively [21].

High-throughput genetic screening for hydrogen sulfide production

Hydrogen sulfide screening was conducted using methylene blue assay as described by Winter G and Curtin C [22] with minor modifications. Briefly, cells were precultured to the stationary phase in 200 μL of YPD (1% yeast extracts, 2% peptone, and 2% glucose) prior to inoculation. Assays were performed in a microtiter plate at a total volume of 250 μL per well.

Each well contained 247 μL of medium and 3% methylene blue reaction mix [23]. The experiments were carried out in triplicate.

Two optical densities were measured: OD_{663} for the hydrogen sulfide indicator and OD_{600} for the cell mass of the wild-type and 3,502 single gene deletion strains. The raw data for hydrogen sulfide production were calculated using the following formula:

Hydrogen sulfide production of strain A = OD_{663} of strain A / OD_{600} of strain A

Selection of genes involved in hydrogen sulfide production under MR condition

To prevent bias from growth defective strains, we eliminated mutant strains exhibiting OD_{600} values less than one-third the wild-type OD_{600} value (Fig. S8). To identify single gene deletion mutants showing lower hydrogen sulfide production than the wild-type under MR condition, we compared the fold-change between mutant and wild-type hydrogen sulfide production and determined the p-value using Student's *t*-test followed by false discovery rate (FDR) adjustment. When the adjusted p-value was less than 0.05 and the fold-change between mutant and wild-type was less than -1.5, genes (137 gene deletion strains; Table S1) were categorized to be significantly involved in hydrogen sulfide production under MR condition. We also compared hydrogen sulfide production in each mutant strain under MR and control conditions. When the ratio of hydrogen sulfide production between the MR and control conditions was less than 1.0 and FDR-adjusted p-value was less than 0.05, genes (81 gene deletion strains; Table S2) were categorized to be significantly involved in hydrogen sulfide increase via MR.

Lead acetate assay

Commercially prepared lead acetate strip papers (Merck Millipore, Germany) or manually prepared lead acetate strip papers (Whatman filter paper soaked in 300 mM lead acetate solution and then dried) were used to detect the hydrogen sulfide emitted from the yeast batch culture. The paper was attached to the culture flask lids and incubated for 1 to 12 h at 30 °C until the paper darkened (due to lead sulfide formation). A color representation from the raw images (Fig. S3) was picked using Photoshop and is presented (Fig. 2b).

Chronological lifespan assay

Lifespan assay was conducted using propidium iodide staining as described previously [24, 25]. Three yeast colonies of each yeast strain were seeded into 10 mL of 2% glucose-containing rich media (YPD) and incubated overnight. The seed culture was re-inoculated into 20 mL of YPD and the yeast cells were grown until the end of the lifespan assay. As the indicated time-point on the viability graph, cells were harvested, washed with phosphate-buffered saline (PBS). And stained with 5 μg/mL of propidium for 20 min at 30 °C. Fluorescence was detected using FACS Verse (BD, USA).

ROS measurement

Cells were harvested at day 6 and incubated in PBS solution containing 50 μM dihydroethidium (Sigma, USA) at 30°C for 20 minutes. Samples were washed thrice with PBS solution and resuspended in 1 mL of PBS. Fluorescence signal was detected in the FL3 channel using flow cytometry (FACSVerse).

Abbreviations

MR: methionine restriction; CR: caloric restriction; TSP: transsulfuration pathway; CBS: cystathionine β-synthase; CGL: cystathionine γ-lyase; CLS: chronological lifespan; ROS: reactive oxygen species; NaHS: sodium hydrosulfide.

AUTHOR CONTRIBUTIONS

Conceived and designed experiments: B.C.L., K.C, and S.K.; performed experiments: K.C., S.K., S.H.K, and H.M.L.; analyzed data: A.K., and C.L.; provided reagents and tools: B.C., Y.K.L., and T.P.; wrote the paper: B.C.L., K.C., S.K., and S.E.

ACKNOWLEDGMENTS

We thank Vadim N. Gladyshev (Harvard Medical School) and Christopher Hine (Harvard School of Public Health) for their valuable discussions and sharing their reagents.

CONFLICTS OF INTEREST

The authors declare no conflicts of interest.

FUNDING

This work was supported by National Research Foundation of Korea (NRF) grants (2018R1A1A1 A05079386, 2018M3A9F3055925) funded by the Korean government (Ministry of Science, ICT & Future Planning) and the Korea University Future Research Grant awarded to B.C.L.

REFERENCES

1. Fontana L, Partridge L, Longo VD. Extending healthy life span--from yeast to humans. Science. 2010; 328:321–26. https://doi.org/10.1126/science.1172539 PMID:20395504

2. Mattison JA, Colman RJ, Beasley TM, Allison DB, Kemnitz JW, Roth GS, Ingram DK, Weindruch R, de Cabo R, Anderson RM. Caloric restriction improves health and survival of rhesus monkeys. Nat Commun. 2017; 8:14063. https://doi.org/10.1038/ncomms14063 PMID:28094793

3. Redman LM, Smith SR, Burton JH, Martin CK, Il'yasova D, Ravussin E. Metabolic Slowing and Reduced Oxidative Damage with Sustained Caloric Restriction Support the Rate of Living and Oxidative Damage Theories of Aging. Cell Metab. 2018; 27:805–815.e4. https://doi.org/10.1016/j.cmet.2018.02.019 PMID:29576535

4. Wu Z, Song L, Liu SQ, Huang D. Independent and additive effects of glutamic acid and methionine on yeast longevity. PLoS One. 2013; 8:e79319. https://doi.org/10.1371/journal.pone.0079319 PMID:24244480

5. Orentreich N, Matias JR, DeFelice A, Zimmerman JA. Low methionine ingestion by rats extends life span. J Nutr. 1993; 123:269–74. PMID:8429371

6. Lee BC, Kaya A, Ma S, Kim G, Gerashchenko MV, Yim SH, Hu Z, Harshman LG, Gladyshev VN. Methionine restriction extends lifespan of Drosophila melanogaster under conditions of low amino-acid status. Nat Commun. 2014; 5:3592. https://doi.org/10.1038/ncomms4592 PMID:24710037

7. Cabreiro F, Au C, Leung KY, Vergara-Irigaray N, Cochemé HM, Noori T, Weinkove D, Schuster E, Greene ND, Gems D. Metformin retards aging in C. elegans by altering microbial folate and methionine metabolism. Cell. 2013; 153:228–39. https://doi.org/10.1016/j.cell.2013.02.035 PMID:23540700

8. Kaeberlein M. Lessons on longevity from budding yeast. Nature. 2010; 464:513–19. https://doi.org/10.1038/nature08981 PMID:20336133

9. Ruckenstuhl C, Netzberger C, Entfellner I, Carmona-Gutierrez D, Kickenweiz T, Stekovic S, Gleixner C, Schmid C, Klug L, Sorgo AG, Eisenberg T, Büttner S, Mariño G, et al. Lifespan extension by methionine restriction requires autophagy-dependent vacuolar acidification. PLoS Genet. 2014; 10:e1004347. https://doi.org/10.1371/journal.pgen.1004347 PMID:24785424

10. Hine C, Harputlugil E, Zhang Y, Ruckenstuhl C, Lee BC, Brace L, Longchamp A, Treviño-Villarreal JH, Mejia P, Ozaki CK, Wang R, Gladyshev VN, Madeo F, et al. Endogenous hydrogen sulfide production is essential for dietary restriction benefits. Cell. 2015; 160:132–44. https://doi.org/10.1016/j.cell.2014.11.048 PMID:25542313

11. Ono B, Shirahige Y, Nanjoh A, Andou N, Ohue H, Ishino-Arao Y. Cysteine biosynthesis in Saccharomyces cerevisiae: mutation that confers cystathionine beta-synthase deficiency. J Bacteriol. 1988; 170:5883–89. https://doi.org/10.1128/jb.170.12.5883-5889.1988 PMID:3056921

12. Ono B, Tanaka K, Naito K, Heike C, Shinoda S, Yamamoto S, Ohmori S, Oshima T, Toh-e A. Cloning and characterization of the CYS3 (CYI1) gene of Saccharomyces cerevisiae. J Bacteriol. 1992; 174:3339–47. https://doi.org/10.1128/jb.174.10.3339-3347.1992 PMID:1577698

13. McIsaac RS, Lewis KN, Gibney PA, Buffenstein R. From yeast to human: exploring the comparative biology of methionine restriction in extending eukaryotic life span. Ann N Y Acad Sci. 2016; 1363:155–70. https://doi.org/10.1111/nyas.13032 PMID:26995762

14. Garay E, Campos SE, González de la Cruz J, Gaspar AP, Jinich A, Deluna A. High-resolution profiling of stationary-phase survival reveals yeast longevity factors and their genetic interactions. PLoS Genet. 2014; 10:e1004168. https://doi.org/10.1371/journal.pgen.1004168 PMID:24586198

15. Perridon BW, Leuvenink HG, Hillebrands JL, van Goor H, Bos EM. The role of hydrogen sulfide in aging and age-related pathologies. Aging (Albany NY). 2016; 8:2264–89. https://doi.org/10.18632/aging.101026 PMID:27683311

16. McIsaac RS, Petti AA, Bussemaker HJ, Botstein D. Perturbation-based analysis and modeling of combinatorial regulation in the yeast sulfur assimilation pathway. Mol Biol Cell. 2012; 23:2993–3007. https://doi.org/10.1091/mbc.e12-03-0232 PMID:22696683

17. Kim HS, Huh J, Fay JC. Dissecting the pleiotropic consequences of a quantitative trait nucleotide. FEMS Yeast Res. 2009; 9:713–22. https://doi.org/10.1111/j.1567-1364.2009.00516.x PMID:19456872

18. Hudson BH, York JD. Roles for nucleotide phosphatases in sulfate assimilation and skeletal disease. Adv Biol Regul. 2012; 52:229–38. https://doi.org/10.1016/j.advenzreg.2011.11.002 PMID:22100882

19. Hancock JT, Whiteman M. Hydrogen sulfide signaling: interactions with nitric oxide and reactive oxygen species. Ann N Y Acad Sci. 2016; 1365:5–14. https://doi.org/10.1111/nyas.12733 PMID:25782612

20. Zheng D, Dong S, Li T, Yang F, Yu X, Wu J, Zhong X, Zhao Y, Wang L, Xu C, Lu F, Zhang W. Exogenous Hydrogen Sulfide Attenuates Cardiac Fibrosis Through Reactive Oxygen Species Signal Pathways in Experimental Diabetes Mellitus Models. Cell Physiol Biochem. 2015; 36:917–29. https://doi.org/10.1159/000430266 PMID:26088607

21. Ham Y, Kim TJ. Anthranilamide from Streptomyces spp. inhibited Xanthomonas oryzae biofilm formation without affecting cell growth. Appl Biol Chem. 2018; 61:673–80. https://doi.org/10.1007/s13765-018-0405-1

22. Winter G, Curtin C. In situ high throughput method for H(2)S detection during micro-scale wine fermentation. J Microbiol Methods. 2012; 91:165–70. https://doi.org/10.1016/j.mimet.2012.08.003 PMID:22981795

23. Lee EJ, Kim GR, Ameer K, Kyung HK, Kwon JH. Application of electron beam irradiation for improving the microbial quality of processed laver products and luminescence detection of irradiated lavers. Appl Biol Chem. 2018; 61:79–89. https://doi.org/10.1007/s13765-017-0338-0

24. Choi KM, Kwon YY, Lee CK. Characterization of global gene expression during assurance of lifespan extension by caloric restriction in budding yeast. Exp Gerontol. 2013; 48:1455–68. https://doi.org/10.1016/j.exger.2013.10.001 PMID:24126084

25. Pu J, Long Y, Zhou J, Zhan YQ, Qin XY. MiR-124 regulates apoptosis in hypoxia-induced human brain microvessel endothelial cells through targeting Bim. Appl Biol Chem. 2018; 61:689–96. https://doi.org/10.1007/s13765-018-0407-z

SUPPLEMENTARY MATERIAL

Supplementary Figures

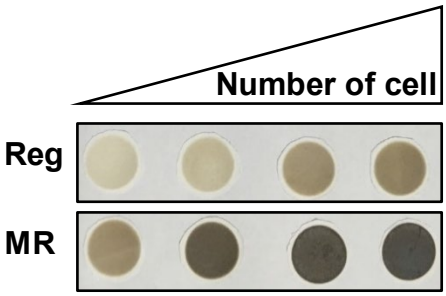

Figure S1. Hydrogen sulfide production by increasing the number of cells under regular (Reg) and MR condition. Hydrogen sulfide was detected by lead acetate method.

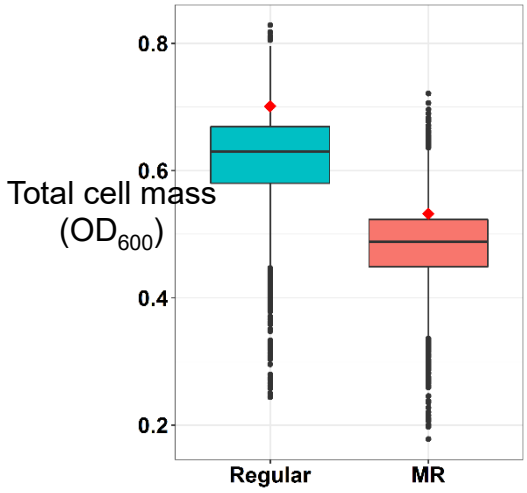

Figure S2. OD_{600} of total screening genes under regular and MR condition at 15 hours after inoculation. The red diamond indicates value for wild-type.

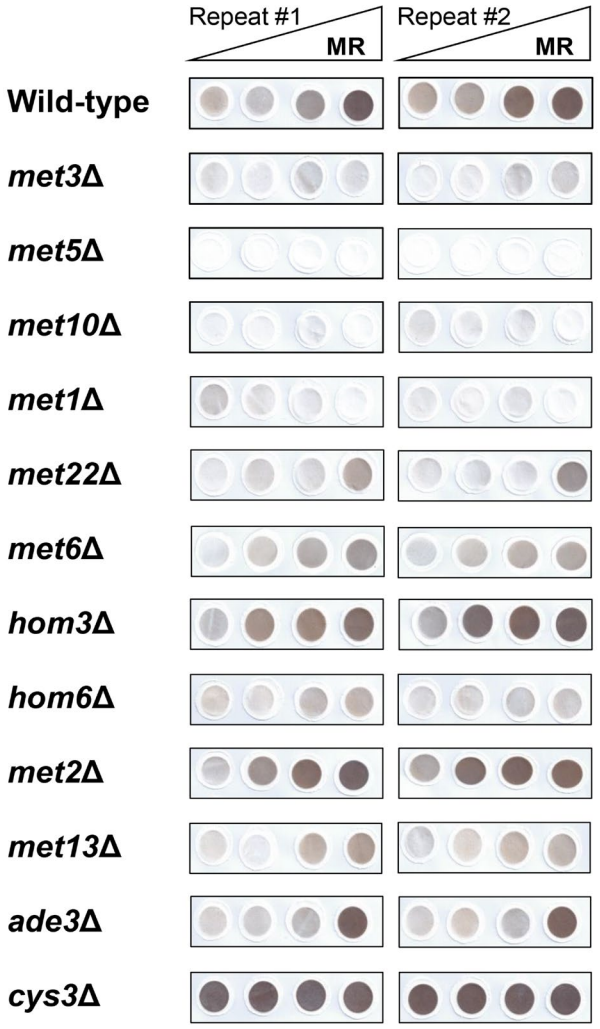

Figure S3. Original images for lead acetate assay in Fig.

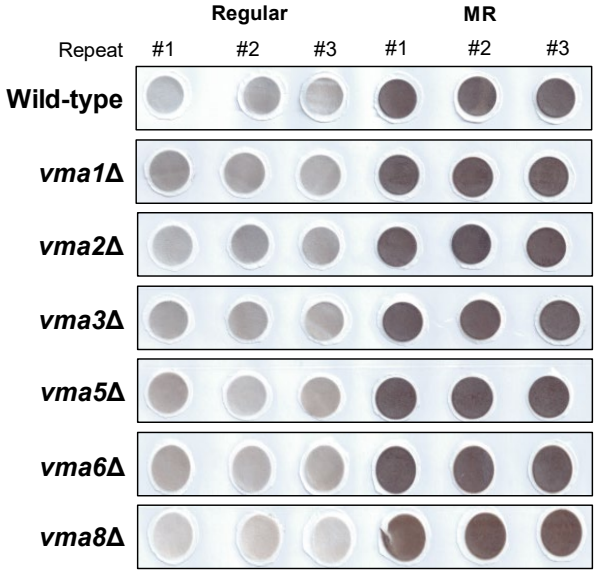

Figure S4. Lead acetate assay for mutants related with vacuolar acidification.

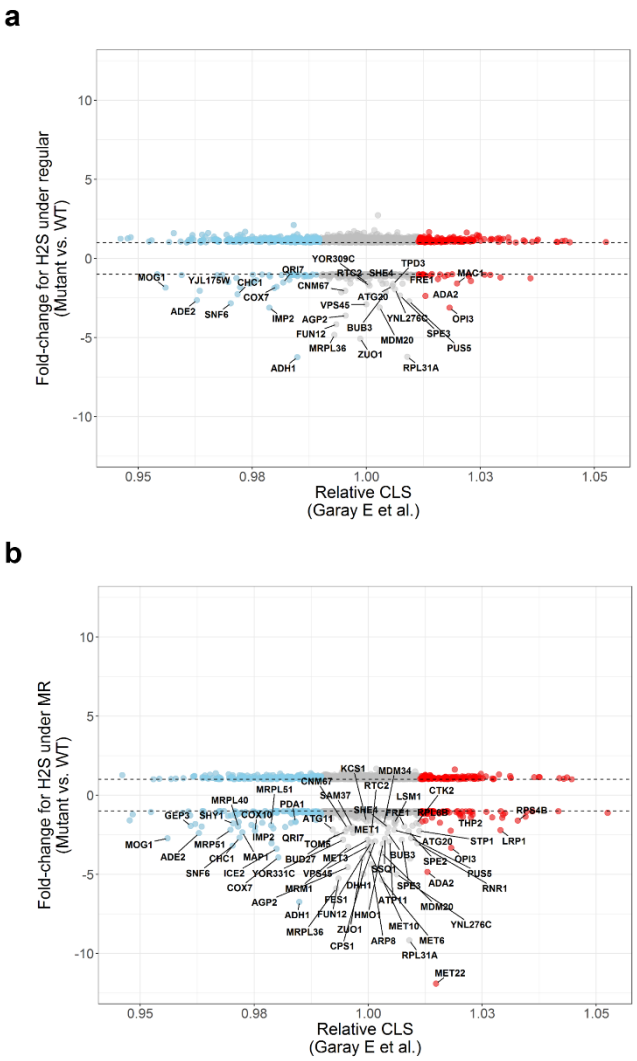

Figure S5. **Comparison between our hydrogen sulfide screening data and chronological lifespan (CLS) screening data by Garay E et al.** Compared to wild-type, change of hydrogen sulfide amount in deletion mutants under regular (a) and MR (b) is depicted. Black dotted line indicates a point where absolute value of fold-change (y axis) is "1". Black label indicates selected genes by comparison between wild-type and mutant under each condition in this study (fold-change < -1.5 and FDR-adj p < 0.05). According to relative CLS, strains with significantly decreased or increased lifespan are shown in blue or red, respectively.

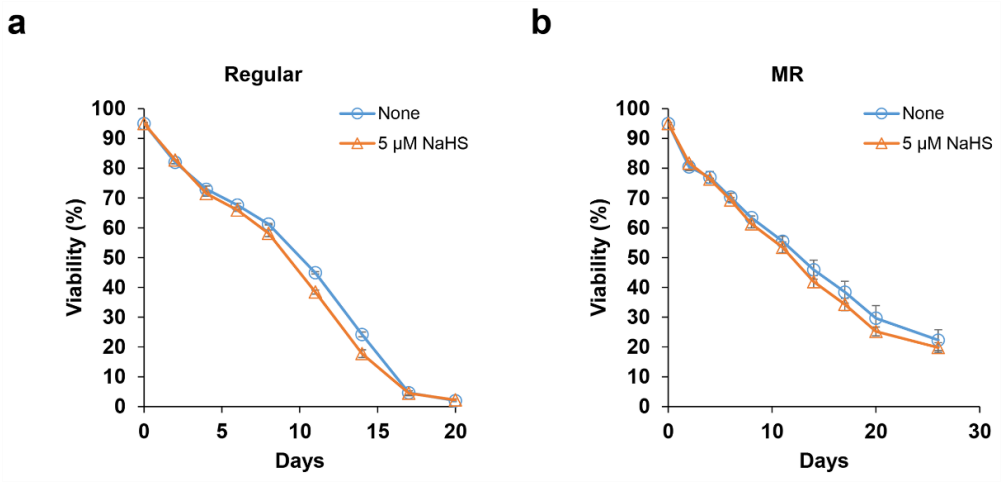

Figure S6. Lifespan under regular (**a**) and MR (**b**) before (blue line) and after (orange line) treating 5 μM NaHS. Graph indicates mean ± SEM.

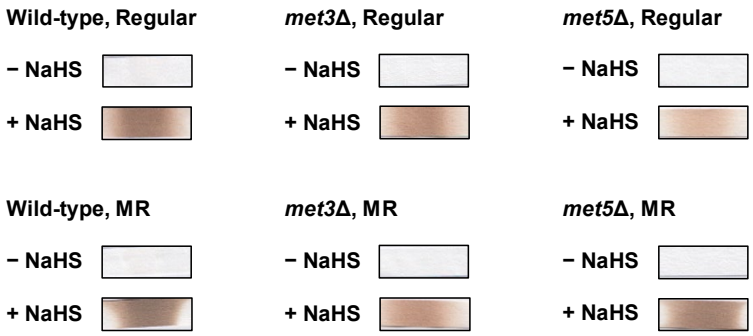

Figure S7. Original images for lead acetate assay in Fig. 4.

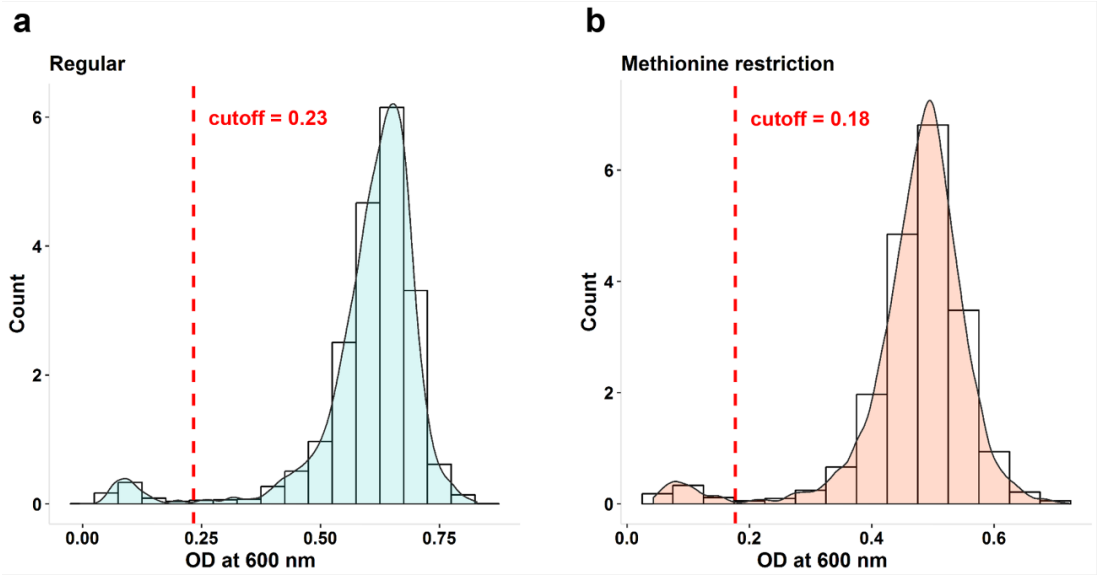

Figure S8. Histogram for OD_{600} of total screening yeast strains under regular (**a**) and MR (**b**). Cells with OD value under a third of wild-type in each condition (below red dotted line) are regarded as the growth-defective.

Supplementary Tables

Table S1. Selected genes by comparison between wild-type and mutant (Analysis 1; 137 genes).

ORF name	Symbol	Fold-change (Mutant vs. Wild-type)	FDR-adj p-value (Mutant vs. Wild-type)
YLR027C	AAT2	-2.6	0.0300
YDR448W	ADA2	-4.9	0.0336
YOR128C	ADE2	-2.4	0.0496
YGR204W	ADE3	-2.0	0.0430
YGR061C	ADE6	-1.5	0.0306
YOL086C	ADH1	-6.7	0.0159
YMR083W	ADH3	-2.0	0.0251
YBR132C	AGP2	-4.5	0.0231
YGL105W	ARC1	-2.2	0.0430
YNL059C	ARP5	-4.5	0.0206
YOR141C	ARP8	-4.4	0.0175
YPR049C	ATG11	-2.2	0.0273
YDL113C	ATG20	-2.2	0.0251
YNL315C	ATP11	-2.9	0.0105
YOR026W	BUB3	-2.4	0.0248
YLR074C	BUD20	-4.4	0.0206
YCR047C	BUD23	-7.4	0.0228
YER014C-A	BUD25	-4.9	0.0170
YFL023W	BUD27	-2.5	0.0418
YGR262C	BUD32	-2.3	0.0357
YER061C	CEM1	-4.0	0.0175
YGL206C	CHC1	-2.7	0.0430
YPL241C	CIN2	-7.0	0.0083
YNL225C	CNM67	-2.1	0.0211
YPL172C	COX10	-2.3	0.0357
YMR256C	COX7	-3.9	0.0293
YJL172W	CPS1	-5.0	0.0210
YKL139W	CTK1	-2.4	0.0404
YJL006C	CTK2	-1.8	0.0228
YAL012W	CYS3	-11.6	0.0426
YKL054C	DEF1	-3.9	0.0206
YDL160C	DHH1	-2.9	0.0216
YCR034W	ELO2	-2.4	0.0306
YBR101C	FES1	-3.0	0.0211
YLR214W	FRE1	-2.0	0.0206
YAL035W	FUN12	-5.3	0.0175
YLR068W	FYV7	-2.5	0.0249
YOR205C	GEP3	-1.9	0.0176
YHR100C	GEP4	-1.5	0.0491
YER083C	GET2	-3.0	0.0032
YEL046C	GLY1	-3.8	0.0085
YGR102C	GTF1	-2.2	0.0494
YDR174W	HMO1	-3.1	0.0228
YER052C	HOM3	-4.7	0.0228

YCR020W-B	HTL1	-2.7	0.0206
YIL090W	ICE2	-3.4	0.0214
YEL044W	IES6	-3.5	0.0362
YMR035W	IMP2	-3.0	0.0231
YDR017C	KCS1	-1.6	0.0323
YFR001W	LOC1	-4.5	0.0083
YHR081W	LRP1	-2.2	0.0261
YJL124C	LSM1	-1.8	0.0367
YDR378C	LSM6	-2.2	0.0418
YKL143W	LTV1	-4.5	0.0175
YLR244C	MAP1	-2.3	0.0379
YOL076W	MDM20	-3.7	0.0211
YGL219C	MDM34	-1.8	0.0468
YKR069W	MET1	-2.4	0.0399
YFR030W	MET10	-3.4	0.0177
YGL125W	MET13	-10.1	0.0166
YIL128W	MET18	-2.7	0.0410
YNL277W	MET2	-6.7	0.0175
YOL064C	MET22	-11.9	0.0175
YJR010W	MET3	-2.8	0.0418
YJR137C	MET5	-2.7	0.0211
YER091C	MET6	-5.4	0.0149
YOR241W	MET7	-4.7	0.0175
YJR077C	MIR1	-1.8	0.0284
YNL076W	MKS1	-3.8	0.0231
YJR074W	MOG1	-2.7	0.0231
YOR201C	MRM1	-3.3	0.0280
YPL118W	MRP51	-2.2	0.0430
YBR122C	MRPL36	-5.9	0.0206
YPL173W	MRPL40	-2.0	0.0418
YPR100W	MRPL51	-1.9	0.0248
YIR021W	MRS1	-4.8	0.0166
YHR120W	MSH1	-3.7	0.0175
YDR432W	NPL3	-3.8	0.0206
YEL062W	NPR2	-2.7	0.0343
YHL023C	NPR3	-3.0	0.0379
YJR073C	OPI3	-3.3	0.0175
YER178W	PDA1	-1.7	0.0275
YOR036W	PEP12	-4.2	0.0121
YNR052C	POP2	-2.4	0.0228
YLR165C	PUS5	-2.7	0.0176
YDL104C	QRI7	-2.0	0.0287
YLR039C	RIC1	-1.8	0.0430
YCR028C-A	RIM1	-8.8	0.0206
YER070W	RNR1	-3.0	0.0382
YMR142C	RPL13B	-2.1	0.0305
YBR191W	RPL21A	-2.8	0.0482
YLR061W	RPL22A	-3.8	0.0125
YHR010W	RPL27A	-4.4	0.0228
YDL075W	RPL31A	-9.2	0.0206
YJL189W	RPL39	-4.5	0.0085

YLR448W	RPL6B	-1.8	0.0460
YDR382W	RPP2B	-2.1	0.0418
YLR048W	RPS0B	-1.9	0.0296
YHR203C	RPS4B	-1.6	0.0454
YOR096W	RPS7A	-3.0	0.0482
YBL025W	RRN10	-2.6	0.0206
YBR147W	RTC2	-2.4	0.0420
YOL067C	RTG1	-3.6	0.0175
YMR060C	SAM37	-2.0	0.0175
YLR403W	SFP1	-2.6	0.0468
YOR035C	SHE4	-2.0	0.0498
YGR112W	SHY1	-1.8	0.0369
YHL025W	SNF6	-3.2	0.0357
YJR104C	SOD1	-1.5	0.0348
YGL127C	SOH1	-1.6	0.0379
YOL052C	SPE2	-2.3	0.0357
YPR069C	SPE3	-2.8	0.0468
YOL148C	SPT20	-3.9	0.0231
YBR081C	SPT7	-2.7	0.0497
YHR041C	SRB2	-2.4	0.0261
YLR369W	SSQ1	-2.7	0.0302
YHR064C	SSZ1	-2.5	0.0228
YDR463W	STP1	-2.3	0.0356
YPL180W	TCO89	-2.0	0.0206
YOL072W	THP1	-4.3	0.0010
YHR167W	THP2	-2.3	0.0486
YPR133W-A	TOM5	-2.3	0.0357
YOR006C	TSR3	-5.7	0.0200
YBR173C	UMP1	-4.6	0.0228
YDL185W	VMA1	-1.8	0.0460
YBR127C	VMA2	-4.0	0.0345
YGR105W	VMA21	-2.3	0.0389
YEL027W	VMA3	-2.7	0.0410
YKL080W	VMA5	-3.4	0.0293
YGL095C	VPS45	-3.2	0.0306
YGR285C	ZUO1	-4.0	0.0287
YNL276C		-5.0	0.0175
YDR521W		-3.5	0.0121
YKL118W		-3.0	0.0265
YOR331C		-2.8	0.0166
YOR200W		-2.3	0.0357
YJR018W		-1.9	0.0273

Table S2. Selected genes by comparison between regular and MR condition (Analysis 2; 81 genes).

ORF name	Symbol	Ratio (MR/Regular)	FDR-adj p-value (MR vs. Regular)
YMR083W	ADH3	0.7	0.0259
YNL059C	ARP5	0.4	0.0043
YPR049C	ATG11	0.7	0.0164
YNL315C	ATP11	0.3	0.0047

YER014C-A	BUD25	0.5	0.0042
YFL023W	BUD27	0.5	0.0135
YLR226W	BUR2	0.6	0.0454
YOR125C	CAT5	0.6	0.0135
YGR062C	COX18	0.8	0.0125
YMR256C	COX7	0.6	0.0202
YJL172W	CPS1	0.2	0.0025
YDL160C	DHH1	0.4	0.0016
YDR069C	DOA4	0.7	0.0476
YGL240W	DOC1	0.7	0.0182
YCR034W	ELO2	0.7	0.0332
YBR101C	FES1	0.5	0.0040
YGR252W	GCN5	0.7	0.0227
YOR205C	GEP3	0.6	0.0152
YHR100C	GEP4	0.5	0.0026
YER040W	GLN3	0.7	0.0132
YOL049W	GSH2	0.5	0.0159
YGR102C	GTF1	0.5	0.0087
YEL059W	HHY1	0.8	0.0359
YER052C	HOM3	0.4	0.0043
YEL044W	IES6	0.4	0.0098
YHR081W	LRP1	0.6	0.0305
YJL124C	LSM1	0.7	0.0076
YOR221C	MCT1	0.7	0.0039
YGL219C	MDM34	0.6	0.0134
YKR069W	MET1	0.5	0.0159
YFR030W	MET10	0.3	0.0016
YGL125W	MET13	0.1	0.0014
YIL128W	MET18	0.4	0.0085
YNL277W	MET2	0.3	0.0039
YOL064C	MET22	0.1	0.0033
YJR010W	MET3	0.5	0.0089
YJR137C	MET5	0.5	0.0040
YER091C	MET6	0.2	0.0042
YOR241W	MET7	0.3	0.0032
YJR077C	MIR1	0.6	0.0290
YGL124C	MON1	0.6	0.0116
YOR201C	MRM1	0.5	0.0247
YKR085C	MRPL20	0.8	0.0333
YPR100W	MRPL51	0.7	0.0314
YDL107W	MSS2	0.9	0.0427
YEL062W	NPR2	0.6	0.0094
YHL023C	NPR3	0.6	0.0372
YER178W	PDA1	0.6	0.0060
YNR052C	POP2	0.7	0.0183
YDL006W	PTC1	0.7	0.0262
YER070W	RNR1	0.5	0.0163
YFL036W	RPO41	0.5	0.0078
YHR203C	RPS4B	0.8	0.0178
YDR502C	SAM2	0.8	0.0135
YCL010C	SGF29	0.5	0.0188

YGR112W	SHY1	0.7	0.0394
YDL047W	SIT4	0.6	0.0127
YCR024C	SLM5	0.9	0.0345
YLR025W	SNF7	0.8	0.0431
YJR104C	SOD1	0.9	0.0332
YOL052C	SPE2	0.6	0.0233
YJL127C	SPT10	0.6	0.0229
YHR178W	STB5	0.6	0.0129
YDR463W	STP1	0.4	0.0183
YCL008C	STP22	0.6	0.0095
YHR167W	THP2	0.5	0.0062
YPR133W-A	TOM5	0.6	0.0142
YOR187W	TUF1	0.7	0.0091
YHR111W	UBA4	0.7	0.0324
YDR470C	UGO1	0.5	0.0100
YBR127C	VMA2	0.6	0.0332
YGR105W	VMA21	0.6	0.0083
YEL027W	VMA3	0.4	0.0070
YLR447C	VMA6	0.6	0.0266
YEL051W	VMA8	0.5	0.0159
YDR080W	VPS41	0.6	0.0293
YML009W-B		0.5	0.0017
YNL276C		0.5	0.0062
YJR018W		0.6	0.0196
YKL118W		0.6	0.0454
YGR219W		0.9	0.0278

Table S3. Median CLS of wild type and deletion mutants on the regular and MR conditions.

Strain	Median CLS on the regular (days)	Median CLS on the MR (days)	p-value (Regular vs. MR)
Wild type	10.1 ± 0.04	13.0 ± 0.95	0.0896
met1Δ	4.9 ± 0.02	12.2 ± 1.37	0.0336
met3Δ	7.2 ± 0.06	23.4 ± 0.18	0.0028
met5Δ	3.2 ± 0.58	20.3 ± 0.78	0.0001
met10Δ	4.9 ± 0.02	13.6 ± 0.84	0.0611

* Data indicate mean ± SEM. P-value was calculated by two-tailed Student's *t*-test.

Table S4. Composition of synthetic complete (SC) media.

Component	**Amount per liter (L)**
Yeast nitrogen base without amino acid	6.7 g
Dextrose	20 g
L-adenine	10 mg
L-arginine	50 mg
L-aspartic acid	80 mg
L-histidine	20 mg
L-isoleucine	50 mg
L-leucine	100 mg

L-lysine	50 mg
L-methionine	50 mg (for regular) or 5 mg (for MR)
L-phenylalanine	50 mg
L-threonine	100 mg
L-tryptophan	50 mg
L-tyrosine	50 mg
L-uracil	20 mg
L-valine	140 mg